Acta Crystallographica Section F
Structural Biology and Crystallization Communications
ISSN 1744-3091

Crystallization, dehydration and preliminary X-ray analysis of excisionase (Xis) proteins cooperatively bound to DNA

My D. Sam,[a] Mohamad A. Abbani,[a] Duilio Cascio,[a] Reid C. Johnson[b] and Robert T. Clubb[a]*

[a]Department of Chemistry and Biochemistry and the UCLA–DOE Center for Genomics and Proteomics, University of California, Los Angeles, 405 Hilgard Avenue, Los Angeles, CA 90095-1570, USA, and [b]Department of Biological Chemistry, UCLA School of Medicine, 10833 Le Conte Avenue, Los Angeles, CA 90095-1737, USA

Correspondence e-mail: rclubb@mbi.ucla.edu

Received 2 June 2006
Accepted 17 July 2006

This paper describes the crystallization, dehydration and preliminary X-ray data analysis of a complex containing several bacteriophage lambda excisionase (Xis) [Bushman *et al.* (1984). *Cell*, **39**, 699–706] proteins cooperatively bound to a 33-mer DNA duplex (Xis–DNA$^{X1\text{-}X2}$). Xis is expected to recognize this regulatory element in a novel manner by cooperatively binding and distorting multiple head-to-tail orientated DNA-binding sites. Crystals of this complex belonged to space group $P3_121$ or $P3_221$, with unit-cell parameters $a = b = 107.7$, $c = 73.5$ Å, $\alpha = \beta = 90$, $\gamma = 120^\circ$. Based on the unit-cell parameters for the asymmetric unit, V_M is 3.0 Å^3 Da^{-1}, which corresponds to a solvent content of ∼59%. The approaches used to crystallize the unusually long DNA fragment in the complex and the dehydration technique applied that dramatically improved the diffraction of the crystals from 10 to 2.6 Å are discussed.

1. Introduction

Bacteriophage lambda uses two highly regulated site-specific DNA-recombination reactions to integrate and excise its genome into and out of its bacterial host's chromosome (Azaro & Landy, 2002). The integration and excision reactions occur within the context of two distinct higher order nucleoprotein complexes (called intasomes) that are assembled by the competitive and cooperative binding of four different proteins to at least 15 DNA sites. The phage-encoded excisionase (Xis) protein is a key regulator of this process, simultaneously stimulating and inhibiting viral excision and integration, respectively (Bushman *et al.*, 1984; Thompson *et al.*, 1987; Moitoso de Vargas & Landy, 1991; Franz & Landy, 1995). It accomplishes this task by cooperatively binding to a regulatory region within the *att*R arm of the prophage that contains two directly repeated sites (X1 and X2), where it stabilizes the excisive intasome structure by bending DNA.

The Xis protein belongs to a large family of recombination directionality factors (Lewis & Hatfull, 2001). The family's name stems from the biological function of its members, which have evolved with their respective recombinases to control the direction of DNA-rearrangement reactions. The lambda Xis protein is the best studied member of the directionality factor family. Previous structural work from our laboratory and from the laboratory of Rüterjans have elucidated the structure of Xis in the absence of DNA by NMR (Sam *et al.*, 2002; Rogov *et al.*, 2003). In addition, our laboratory has determined the X-ray structure of a single Xis protein bound to site X2 (Sam *et al.*, 2004). However, this work failed to reveal how Xis cooperatively binds and distorts the X1-X2 region. The mode of cooperative binding to these sites must be unusual because they are arranged in a head-to-head configuration, which necessitates that multiple proteins assemble to form an asymmetric complex. This contrasts with nearly all other sequence-specific DNA-binding proteins, which typically cooperatively bind DNA by forming symmetrical oligomers that interact with DNA palindromes (head-to-head orientated binding sites; Luisi *et al.*, 1991; Schwabe *et al.*, 1993). As a step towards understanding this intriguing mode of DNA binding, we report the crystallization and dehydration techniques

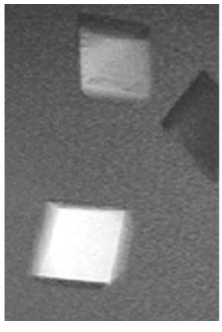

used to obtain high-quality crystals of several Xis proteins bound to a 33-mer DNA duplex containing sites X1 and X2 (the Xis–DNA$^{X1\text{-}X2}$ complex).

2. Methods

2.1. Purification of the Xis protein and DNA substrates

The Xis protein (residues 1–55 with a Cys-to-Ser mutation at position 28) was expressed and purified from Bl21(DE3) as previously described (Sam *et al.*, 2002). This protein contained the minimal DNA-binding domain (Numrych *et al.*, 1992; Wu *et al.*, 1998) and is sufficient for cooperative binding to the Xis regulatory region (Sam *et al.*, 2002). DNA was purchased from Biosource International and was purified on 17% (for DNA lengths $\geq$ 20 nucleotides) or 20% (for DNA lengths $\leq$ 20 nucleotides) acrylamide–urea gels [bis-acrylamide (37.5:1) containing 7 *M* urea dissolved in 1× TBE (Tris–borate–EDTA) buffer]. A typical sequencing gel was used (32 × 41 cm) with a 2.2 mm thick spacer. The gel had a loading capacity of 5–10 mg ssDNA. The gels were run at constant power (30–50 W) for 10–15 h depending on DNA length. The migration of the DNA was gauged by loading bromophenol blue and xylene cyanol dyes onto the outer edges of the gel. The separated DNA gel was then placed on TLC (thin layer chromatography) plates (Whatman, PE SIL G/UV flexible plates) and visualized with a handheld UV lamp (λ = 254 nm). After excision, the gel fragments containing the DNA were cut into small pieces and loaded onto an Elutrap Electro-Elution System running at constant voltage (150 V) in 1× TBE buffer. The eluted DNA from the gel pieces was trapped in a small chamber gated by dialysis membranes at the anode end of the elute-trap device. Once all DNA had been eluted from the gel pieces (~8 h), the urea, unpolymerized acrylamide and TBE buffer were exchanged with 50 m*M* sodium acetate pH 5.5, 100 m*M* NaCl and 2 m*M* EDTA through dialysis. The DNA used to successfully crystallize the complex was generated by annealing three complementary strands (one bottom and two shorter top strands). This gave a duplex DNA with a single nick on the top strand, which presumably relieves strain when the DNA is distorted from the B form by Xis binding (Fig. 1*a*). Prior to crystallization trials, purified Xis protein and dsDNA were stored at 277 K in 25 m*M* sodium acetate pH 5.5, 100 m*M* NaCl and 2 m*M* EDTA at concentrations ranging between 50 and 150 μ*M*.

2.2. Complex formation

The number of Xis proteins that bind to the DNA molecule is not known. A minimum of two Xis proteins should bind to sites X1 and X2, but it is possible that an additional Xis protein binds to the seven-base-pair sequence that separates the two sites (Fig. 1*a*). In the crystallization trials, we elected to use a molar ratio of two Xis proteins to 1.2 DNA molecules because Xis has a high propensity to form protein-only crystals even in the presence of DNA. Although this could in principle have led to a heterogeneous mixture in which the duplex was only partially occupied by the protein, the crystallization process captures a single species of the complex that has a defined stoichiometry (demonstrated in Fig. 1*c*). The solution of the complex was clear of precipitates and was dialyzed into 25 m*M* sodium acetate pH 5.5 to remove all traces of NaCl. The Xis–DNA$^{X1\text{-}X2}$ complex was then concentrated to 10–12 mg ml^{-1} and screened for crystal growth using the hanging-drop diffusion method.

3. Results

3.1. Crystal screening

Complexes containing six distinct DNA constructs were screened for crystal growth. Each DNA fragment harbored sites X1 and X2, but differed in their length and/or the presence of overhangs. This strategy was used because systematic variation of these parameters has been successfully employed by others to obtain highly ordered protein–DNA cocrystals (Jordan *et al.*, 1985; Tan *et al.*, 2000). Complexes were then subjected to sparse-matrix crystal screening

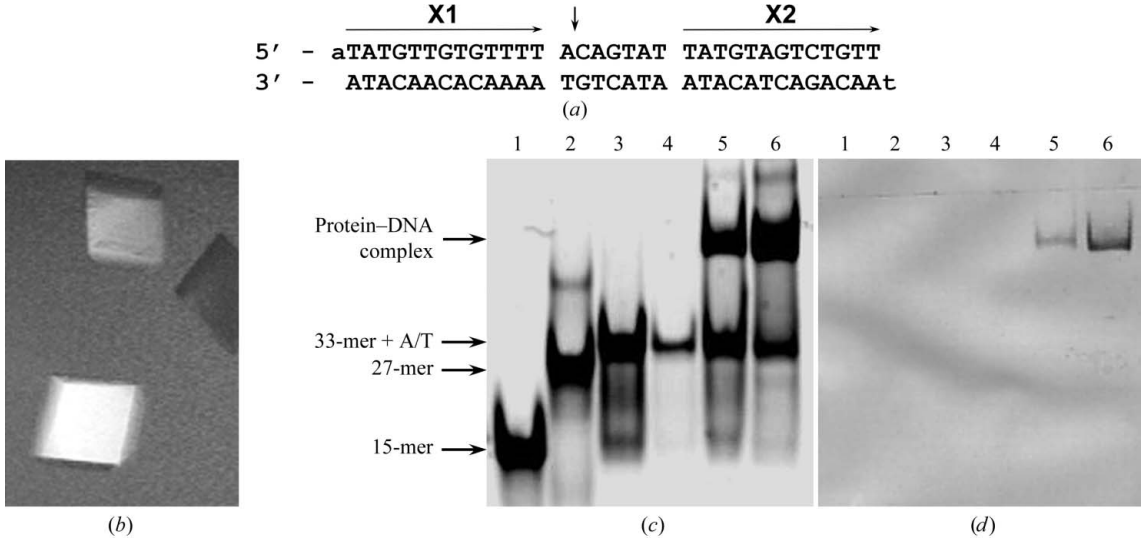

Figure 1
(*a*) Sequence of the 33-mer dsDNA with an A/T overhang used to grow crystals of the Xis–DNA$^{X1\text{-}X2}$ complex. Two tandem unique Xis-binding sites are denoted X1 and X2. This dsDNA was formed by mixing three complementary strands to produce a nick within the top strand that is indicated by an arrow. (*b*) Tetragonal shaped native Xis–DNA$^{X1\text{-}X2}$ crystals grown in 30% PEG 4K, 0.2 *M* ammonium acetate, 0.1 *M* sodium citrate pH 6.2 and ~10 mg ml^{-1} of the complex. (*c*) 15% native polyacrylamide gel stained to only visualize nucleic acids (SYBR-Gold nucleic acid stain). Lanes 1–4 are loading standards and include a 15-mer (1 µg), a 27-mer (1 µg), a 33-mer with A/T overhang (1 µg) and a 33-mer with A/T overhang (0.1 µg) dsDNA, respectively. Two crystals from (*b*) were isolated, washed, dissolved and loaded onto lanes 5 and 6. (*d*) The same native gel from (*c*) was washed and selectively stained for protein with Coomassie Blue protein stain. The presence of retarded mobility bands in lanes 5 and 6 indicate that the crystals contain the protein–DNA complex.

using Hampton Research Crystal Screens 1 and 2 and each potential crystal lead was optimized by varying the pH, salt and precipitant concentration. In order to verify the presence of both protein and DNA in the crystals, the contents of individual crystals were resolved on a 15% native acrylamide gel (Figs. 1*c* and 1*d*). It should be noted that confirmation by gel electrophoresis was critical, since many crystals contained only Xis protein. Moreover, the migration of the shifted species confirms that at least two Xis proteins are cooperatively bound to sites X1 and X2.

Reproducible crystals were grown using the 33 bp sequence containing an A/T overhang (Fig. 1*a*). The crystals were grown in 30% PEG 4K, 0.2 *M* ammonium acetate and 0.1 *M* sodium citrate pH 5.6 over a period of three months. Optimized conditions in which the pH of the sodium citrate was raised to 6.2 gave crystals that grew to dimensions of 0.2 × 0.2 × 0.2 mm in as little as a week (Fig. 1*b*).

3.2. Crystal diffraction and dehydration

The initial crystals of the Xis–DNA$^{X1\text{-}X2}$ complex only diffracted to 10 Å (Fig. 2*a*). Hampton Research Additive Screens I–III and application of an annealing protocol failed to improve the crystal diffraction quality. The latter method transiently returns the flash-cooled crystal to ambient temperature and has been shown to improve poor resolution and mosaicity presumably caused by flash-cooling (Harp *et al.*, 1998; Kriminski *et al.*, 2002). To test whether the nick on the top strand of the duplex was responsible for poor crystal packing, new complexes that moved the nick to the bottom strand were crystallized, but these alternate complexes did not show improved diffraction quality. Fortunately, crystal dehydration dramatically improved crystal quality (Kuo *et al.*, 2003; Haebel *et al.*, 2001; Tong *et al.*, 1997). The conditions used to cryoprotect the crystals were identical to those used for the non-dehydrated crystals and involved the addition of glycerol to the mother liquor (to a final concentration of 20% glycerol). Xis–DNA$^{X1\text{-}X2}$ crystals were dehydrated by replacing both the well and hanging-drop solutions with a solution that contained the mother liquor plus 5–10% more precipitant (PEG 4K in this case). The hanging drop containing the crystals was then allowed to dehydrate for 2–3 d. Dehydration at 289 K significantly improved the diffraction from 10 to ∼3 Å (Fig. 2*b*), but the results were not reproducible, since only one out of ten crystals showed improvement to the 3 Å resolution limit and these crystals had variable unit-cell parameters (two crystal forms were observed with parameters $a = b = 107.7$, $c = 73.5$ Å or $a = b = 112.3$, $c = 78.0$ Å). Furthermore, these crystals gave somewhat anisotropic X-ray diffraction, which suggested that they had not been uniformly dehydrated. This idea is consistent with the observation that after dehydration crystals that are larger than 0.2 × 0.2 × 0.2 mm did not diffract to 3 Å, presumably because larger crystals are more difficult to dehydrate uniformly. To obtain more uniformly diffracting crystals, they were dehydrated at 277 K, which resulted in more isotropic crystals and further improved the diffraction quality by ∼0.2–0.4 Å (Fig. 2*c*). However, as with dehydration at 289 K, this approach also required multiple attempts, as only one out of ten crystals showed diffraction improvement beyond 3 Å. It is possible that the diffraction exhibited by larger crystals selectively deteriorates as a result of the cryoprotection process. However, this seems unlikely as the same conditions were used to cryoprotect all of the crystals and only those crystals that were dehydrated showed improved diffraction.

3.3. Preliminary X-ray analysis

A 2.6 Å Bragg spacing native data set was collected at the synchrotron and the intensity data were indexed, integrated and scaled using the *HKL* programs *DENZO* and *SCALEPACK* (Otwinowski *et al.* 1997). The unit-cell parameters for this crystal are $a = b = 107.7$, $c = 73.5$ Å, $\alpha = \beta = 90$, $\gamma = 120^\circ$ in space group $P3_121$ or $P3_221$ (complete statistics are listed in Table 1). Extensive efforts to solve the structure of the Xis–DNA$^{X1\text{-}X2}$ complex using the published structure of the single Xis–DNA complex as a search model have proven unsuccessful [methods attempted included *EPMR* (Kissinger *et al.*, 1999), *AMoRe* (Navaza, 1994), *MOLREP* (Vagin *et al.*, 2000) and *Phaser* (Storoni *et al.*, 2004)]. Failure to find a solution suggests that there are substantial structural differences between the single-Xis and multi-Xis DNA–protein complexes, which is not surprising as biochemical experiments indicate that at least two Xis proteins cooperatively bind to and dramatically distort the DNA duplex. Although it is possible that the structure of the complex will change upon dehydration, we believe that substantial changes are unlikely. Our current work is focused on obtaining phase information through application of the MIRAS or MAD methods to complexes in which

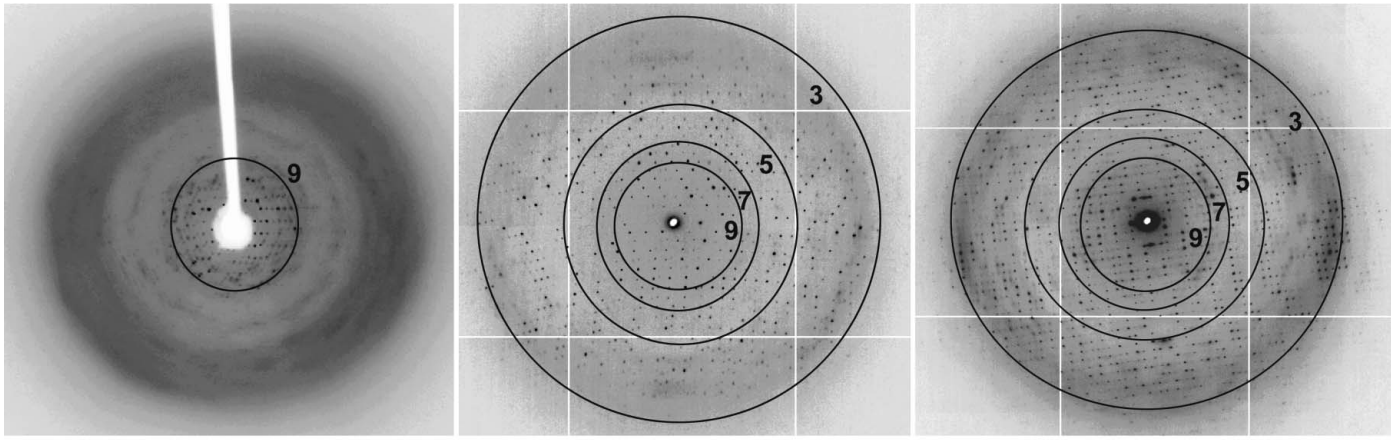

Figure 2
(*a*) A typical 1° oscillation diffraction image of the Xis–DNA$^{X1\text{-}X2}$ complex prior to dehydration, showing that the reflections only extend to ∼9–10 Å. (*b*) The crystals were dehydrated by replacing the well and hanging-drop solutions with a solution containing the mother liquor plus 5–10% more precipitant (PEG 4K) and allowing it to equilibrate at 289 K for 2–3 d. As shown in this diffraction image, the dehydrated crystal diffracted to ∼3 Å. (*c*) Further fine-tuning this dehydration technique by allowing the crystals to dehydrate at 277 K gave more isotropic diffraction with a 0.2–0.4 Å increase in the resolution limit.

Table 1
X-ray crystallographic parameters and data-collection statistics.

Values in parentheses are for the highest resolution shell.

Beamline	ALS Berkeley
Wavelength (Å)	0.9197
Space group	$P3_121/P3_221$
Unit-cell parameters (Å, °)	$a = b = 107.7$, $c = 73.5$, $\alpha = \beta = 90$, $\gamma = 120$
Matthews coefficient (Å^3 Da^{-1})	3.0
Molecules per ASU	1.0
Solvent content (%)	59
Resolution (Å)	100–2.6 (2.69–2.60)
No. of observations	106944 (10926)
No. unique observations	15456 (1509)
Completeness (%)	99.9 (100.0
R_{sym}†	0.079 (0.451)
$\langle I/\sigma(I)\rangle$‡	24.1 (5.1)

† $R_{sym} = \sum_{hkl}\sum_i |I_i(hkl) - \langle I(hkl)\rangle| / \sum_{hkl}\sum_i I_i(hkl)$, where I_i is the ith measurement of reflection $I(hkl)$. ‡ $\langle I/\sigma(I)\rangle$ is the mean reflection intensity divided by the estimated error of the intensity.

the thymine bases are replaced with 5-iodouracil or 5-bromouracil, respectively. Preliminary crystallization trials of complexes containing these thymine derivatives have yielded crystals that diffract to high resolution after application of our dehydration technique and we are therefore confident that these approaches will prove successful.

We thank Mr Carlos Lopez for his assistance with crystallizing and dehydrating several of the complexes.

References

Azaro, M. A. & Landy, A. (2002). *Mobile DNA II*, edited by N. L. Craig, R. Craigie, M. Gellert & A. M. Lambowitz, pp. 118–148. Washington, DC: ASM Press.

Bushman, W., Yin, S., Thio, L. L. & Landy, A. (1984). *Cell*, **39**, 699–706.

Franz, B. & Landy, A. (1995). *EMBO J.* **14**, 397–406.

Haebel, P. W., Wichman, S., Goldstone, D. & Metcalf, P. (2001). *J. Struct. Biol.* **136**, 162–166.

Harp, J. M., Timm, D. E. & Bunick, G. J. (1998). *Acta Cryst.* D**54**, 622–628.

Jordan, S. R., Whitcombe, T. V., Berg, J. M. & Pabo, C. O. (1985). *Science*, **230**, 1383–1385.

Kissinger, C. R., Gehlhaar, D. K. & Fogel, D. B. (1999). *Acta Cryst.* D**55**, 484–491.

Kriminski, S., Caylor, C. L., Nonato, M. C., Finkelstein, K. D. & Thorne, R. E. (2002). *Acta Cryst.* D**58**, 459–471.

Kuo, A., Bowler, M. W., Zimmer, J., Antcliff, J. F. & Doyle, D. A. (2003). *J. Struct. Biol.* **141**, 97–102.

Lewis, J. A. & Hatfull, G. F. (2001). *Nucleic Acids Res.* **29**, 2205–2216.

Luisi, B. F., Xu, W. X., Otwinowski, Z., Freedman, L. P., Yamamoto, K. R. & Sigler, P. B. (1991). *Nature (London)*, **352**, 497–505.

Moitoso de Vargas, L. & Landy, A. (1991). *Proc. Natl Acad. Sci. USA*, **88**, 588–592.

Navaza, J. (1994). *Acta Cryst.* A**50**, 157–163.

Numrych, T. E., Gumport, R. I. & Gardner, J. F. (1992). *EMBO J.* **11**, 3797–3806.

Otwinowski, Z. & Minor, W. (1997). *Methods Enzymol.* **276**, 307–326.

Rogov, V. V., Lucke, C., Muresanu, L., Wienk, H., Kleinhaus, I., Werner, K., Lohr, F., Pristovsek, P. & Rüterjans, H. (2003). *Eur. J. Biochem.* **270**, 4846–4858.

Sam, M. D., Cascio, D., Johnson, R. C. & Clubb, R. T. (2004). *J. Mol. Biol.* **338**, 229–240.

Sam, M. D., Papagiannis, C., Connolly, K. M., Corselli, L., Iwahara, J., Lee, J., Phillips, M., Wojciak, J. M., Johnson, R. C. & Clubb, R. T. (2002). *J. Mol. Biol.* **324**, 791–805.

Schwabe, J. W., Chapman, L., Finch, J. T. & Rhodes, D. (1993). *Cell*, **75**, 567–578.

Storoni, L. C., McCoy, A. J. & Read, R. J. (2004). *Acta Cryst.* D**60**, 432–438.

Tan, S., Hunziker, Y., Pellegrini, L. & Richmond, T. J. (2000). *J. Mol. Biol.* **297**, 947–059.

Thompson, J. F., Moitoso de Vargas, L., Koch, C., Kahmann, R. & Landy, A. (1987). *Cell*, **50**, 901–908.

Tong, L., Qian, C., Davidson, W., Massariol, M. J., Bonneau, P. R., Cordingley, M. G. & Lagace, L. (1997). *Acta Cryst.* D**53**, 682–690.

Vagin, A. & Teplyakov, A. (2000). *Acta Cryst.* D**56**, 1622–1624.

Wu, Z., Gumport, R. I. & Gardner, J. F. (1998). *J. Mol. Biol.* **281**, 651–661.